



Minnesota  
Department of  
Transportation

# Improved Approach to Enforcement of Road Weight Restrictions

**RESEARCH  
SERVICES  
AND  
LIBRARY**

**Office of  
Transportation  
System  
Management**

Rajesh Rajamani, Principal Investigator  
Department of Mechanical Engineering  
University of Minnesota

**November 2013**

Research Project  
Final Report 2013-27



*Your Destination... Our Priority*



To request this document in an alternative format call [651-366-4718](tel:651-366-4718) or [1-800-657-3774](tel:1-800-657-3774) (Greater Minnesota) or email your request to [ADArequest.dot@state.mn.us](mailto:ADArequest.dot@state.mn.us). Please request at least one week in advance.

## Technical Report Documentation Page

1. Report No. MN/RC 2013-27	2.	3. Recipients Accession No.	
4. Title and Subtitle Improved Approach to Enforcement of Road Weight Restrictions		5. Report Date November 2013	
7. Author(s) Lee Alexander, Gridsada Phanomchoeng and Rajesh Rajamani		6.	
9. Performing Organization Name and Address Department of Mechanical Engineering University of Minnesota 111 Church Street SE Minneapolis, MN 55455		8. Performing Organization Report No.	
12. Sponsoring Organization Name and Address Minnesota Local Road Research Board Minnesota Department of Transportation Research Services and Library 395 John Ireland Boulevard, MS 330 St. Paul, MN 55155		10. Project/Task/Work Unit No. CTS Project # 2012005	
		11. Contract (C) or Grant (G) No. (C) 99008 (WO) 13	
15. Supplementary Notes <a href="http://www.lrrb.org/pdf/201327.pdf">http://www.lrrb.org/pdf/201327.pdf</a>		13. Type of Report and Period Covered Final Report	
		14. Sponsoring Agency Code	
16. Abstract (Limit: 250 words) <p>This project focused on the enhancement and evaluation of a battery-less wireless weigh-in-motion (WIM) sensor for improved enforcement of road weight restrictions. The WIM sensor is based on a previously developed vibration energy harvesting system, in which energy is harvested from the vibrations induced by each passing vehicle to power the sensor.</p> <p>The sensor was re-designed in this project so as to reduce its height, allow it to be installed and grouted in an asphalt pavement, and to protect the piezo stacks and other components from heavy shock loads. Two types of software interfaces were developed in the project:</p> <ul style="list-style-type: none"> <li>a) An interface from which the signals could be read on the MnDOT intranet</li> <li>b) An interface through a wireless handheld display</li> </ul> <p>Tests were conducted at MnRoad with a number of test vehicles, including a semi tractor-trailer at a number of speeds from 10 to 50 mph. The sensor had a monotonically increasing response with vehicle weight. There was significant variability in sensor response from one test to another, especially at the higher vehicle speeds. This variability could be attributed to truck suspension vibrations, since accelerometer measurements on the truck showed significant vibrations, especially at higher vehicle speeds. MnDOT decided that the final size of the sensor was too big and could pose a hazard to the traveling public if it got dislodged from the road. Hence the task on evaluation of the sensor at a real-world traffic location was abandoned and the budget for the project correspondingly reduced.</p>			
17. Document Analysis/Descriptors Weigh in motion, Road sensor, Sensors, Systems of measurement, Heavy truck weights, Energy harvesting		18. Availability Statement No restrictions. Document available from: National Technical Information Services, Alexandria, Virginia 22312	
19. Security Class (this report) Unclassified	20. Security Class (this page) Unclassified	21. No. of Pages 45	22. Price

# **Improved Approach to Enforcement of Road Weight Restrictions**

## **Final Report**

*Prepared by:*

Lee Alexander  
Gridsada Phanomchoeng  
Rajesh Rajamani

Department of Mechanical Engineering  
University of Minnesota

**November 2013**

*Published by:*

Minnesota Department of Transportation  
Research Services and Library  
395 John Ireland Boulevard, MS 330  
St. Paul, Minnesota 55155-1899

This report represents the results of research conducted by the authors and does not necessarily represent the views or policies of the Minnesota Local Road Research Board, the Minnesota Department of Transportation or the University of Minnesota. This report does not contain a standard or specified technique.

The authors, the Minnesota Local Road Research Board, the Minnesota Department of Transportation, and the University of Minnesota, do not endorse products or manufacturers. Any trade or manufacturers' names that may appear herein do so solely because they are considered essential to this report.

# Table of Contents

I. Introduction	1
II. AMR Sensors for Vehicle Detection	2
2.1 Vehicle Detection	2
2.2 Vehicle Speed Calculation	2
2.3 Vehicle Classification	3
2.4 Summary	8
2.5 Appendix: Sample Magnetic Signals	9
III. WIM Sensor Redesign	14
3.1 Introduction	14
3.2 First Generation Redesign	14
3.3 Performance of First Generation Sensor	16
3.4 Second Generation Sensor Redesign	21
IV. Electronic and Software Interfaces	24
4.1 Electronics Inside WIM Sensor	24
4.2 Software Interfaces	25
V. Experimental Results	29
5.1 Sensor Grouting in Pavement	29
5.2 Axle Weight Readings	30
5.3 Truck Vibrations	31
5.4 Summary	34
VI. Conclusions	35
References	36

## List of Figures

Figure 2.1: PCB with two AMR sensors, microprocessor and wireless transceiver system	2
Figure 2.2: Vehicle lengths estimated by AMR Sensors	7
Figure 2.3: Vehicle lengths estimated by AMR Sensors	7
Figure 2.4: AMR sensor signals with a Mazda Protégé passenger sedan	9
Figure 2.5: AMR sensor signals with a Ford Ranger small pick-up truck	10
Figure 2.6: AMR sensor signals with a Ford Econoline E-Series van	11
Figure 2.7: AMR sensor signals with a snowplow	12
Figure 2.8: AMR sensor signals with a semi tractor-trailer	13
Figure 3.1: Sensor re-design to move legs into main body of sensor	14
Figure 3.2: Schematic of sensor operation	15
Figure 3.3: First generation sensor leg design	16
Figure 3.4: Mazda Protégé sedan used for testing and its sensor response	16
Figure 3.5: Ford ranger pick-up used for testing and its sensor response	17
Figure 3.6: Large Ford pick-up truck used for testing and its sensor response	17
Figure 3.7: Ford E-series full size van used for testing and its sensor response	18
Figure 3.8: Snowplow truck used for testing and its sensor response	18
Figure 3.9: Semi tractor-trailer used for testing and its sensor response	19
Figure 3.10: Sensor signal as a function of vehicle weight	19
Figure 3.11: Failures in piezo stack due to semi tractor-trailer loads	20
Figure 3.12: Failures in piezo stack due to semi tractor-trailer loads	21
Figure 3.13: Original leg design (first generation)	21
Figure 3.14: Second generation sensor leg design	22
Figure 3.15: Details of new sensor leg design	22
Figure 3.16: Overall design of 2nd generation sensor showing legs inside main body	23
Figure 4.1: Energy harvesting circuit that interfaces with piezoelectric stack	24
Figure 4.2: Weight measurement circuit that uses piezo film and charge amplifier circuit	25
Figure 4.3: Major interface components for access to WIM sensor	26
Figure 4.4: Showing internals of interface components for WIM sensor	26
Figure 4.5: Close-up of wireless handheld display	27
Figure 4.6: Downloaded file of WIM sensor readings	28
Figure 5.1: Photograph of sensor in external box that has been grouted in asphalt pavement	30
Figure 5.2: Half Axle weight measurements for various vehicles at speeds from 10 – 40 mph	31
Figure 5.3: Half Axle weight measurements for various vehicles at speeds from 10 – 50 mph	32
Figure 5.4: Axle vibrations on semi-truck at 10 mph	33
Figure 5.5: Axle vibrations on semi-truck at 20 mph	33
Figure 5.6: Axle vibrations on semi-truck at 30 mph	34
Figure 5.7: Axle vibrations on semi-truck at 40 mph	34
Figure 5.8: Axle vibrations on semi-truck at 50 mph	37

## **List of Tables**

Table 2.1: Vehicle Velocity Estimation and Reference Sonar Sensor	5
Table 2.2: Vehicle Velocity Estimation with More Accurate Reference Sensor	6
Table 2.3: Vehicle Magnetic Lengths	7

## Executive Summary

This project focused on the enhancement and evaluation of a battery-less, wireless weigh-in-motion (WIM) sensor for improved enforcement of road weight restrictions. The WIM sensor is based on a previously developed vibration energy harvesting system, in which energy is harvested from the vibrations induced by each passing vehicle to power the sensor.

The sensor was re-designed in this project so as to

- 1) Reduce its height to 3.5 inches, which allowed it to be installed in an asphalt pavement
- 2) Allow its enclosure in a metal casing, which could be grouted to the pavement
- 3) Protect the piezo stacks in the sensor from overloading by heavy trucks while still allowing adequate energy to be harvested from light vehicles. This was achieved by using a novel combination of parallel and series spring elements.
- 4) Protect the piezo film used for weight measurement from overloads while still allowing it to experience a force proportional to vehicle weight.
- 5) Protect the electronics in the sensor from large voltage spikes caused by high-speed heavy truck loads.
- 6) Provide software interfaces for easy access to readings from the WIM sensor.

Two types of software interfaces were developed in the project:

- a) An interface through an existing International Road Dynamics IRD (IRD) controller box, from which the signals could be read on the MnDOT intranet
- b) An interface through a wireless handheld display, from which WIM signals could be read in the neighborhood of the sensor.

Tests were conducted at MnROAD with a number of test vehicles, including a semi tractor-trailer at a number of speeds from 10 to 50 mph. The sensor had a monotonically increasing response with vehicle weight. There was significant variability in sensor response from one test to another, especially at the higher vehicle speeds. This variability could be attributed to truck suspension vibrations, since accelerometer measurements on the truck showed significant vibrations, especially at higher vehicle speeds.

There was unexplained loss of data for the reading from the first axle of the semi tractor-trailer on several occasions. This loss of data could not be explained. It was not due to inadequate energy harvesting, since the energy harvesting system provided adequate energy from the first axle for several vehicles that were much lighter.

MnDOT decided that the final size of the sensor was too big and could pose a hazard to the traveling public if it got dislodged from the road. Hence the task on evaluation of the sensor at a real-world traffic location was abandoned and the budget for the project correspondingly reduced.



## I. INTRODUCTION

The overarching goal of this project is to develop an improved approach to road weight restriction enforcement based on a battery-less, wireless weigh-in-motion sensor.

In a previous research project [2], a battery-less, wireless weigh-in-motion (WIM) sensor was developed by this research team. The sensor was inexpensive and the cost of materials for the sensor was only \$200. Energy for its operation was entirely obtained from vibrations induced by each passing vehicle [1]. The final size of the sensor was 6 feet long x 10 inches wide x 5 inches deep. It transmitted weight information to a roadside receiver.

In the workplan for this project, the sensor was to be enhanced so as to enable it to calculate the total weight of the truck accurately. Earlier the WIM sensor could measure axle weight. However, at low vehicle speeds, the sensor was unable to reliably identify which axles belong to which vehicle. At low vehicle speeds, the distance between vehicles can be small. There was no method available to identify whether consecutive axles belong to one vehicle or to consecutive vehicles.

The work in the project proposed to add an Anisotropic Magnetoresistive (AMR) device to the WIM sensor. An AMR sensor responds to the magnetic field of each vehicle (just like an inductive loop). AMR sensors are currently already being used as traffic sensors. AMR sensors cannot measure the number of axles or the weight of any axle. However, they can reliably count vehicles, differentiating one consecutive vehicle from another. The addition of AMR sensors to the current WIM sensor would enable it to calculate the total weight of each passing vehicle.

The workplan for the project also included enhancement of the sensor design so as to enable it to be embedded in the road. The previous sensor had only been tested by wedging it into a slot in the road. If the sensor were to be grouted to the road, it would have a stiff connection with the road. A portion of the load on the sensor would be expended in deflecting the sensor with respect to the road, i.e. in overcoming the resistance of the grout. This would cause the weight of the vehicle to be under-estimated and would also result in less energy harvested for sensor operation. The sensor design needed to be enhanced to address these issues.

Another shortcoming of the sensor was that its height of 5 inches only enabled it to be used in a concrete road. In order to enable the sensor to be used in an asphalt road, its height needed to be reduced to 3.5 inches.

Finally, the sensor had reliability issues with its electronics and these issues needed to be addressed.

The performance of the enhanced WIM sensor was planned to be first verified at MnROAD. The original workplan also had a task related to evaluation of the sensor at a real-world traffic location. The sensor would have two types of interfaces:

- a) An interface with through an existing IRD WIM controller box so as to provide Internet access over MnDOT's intranet.
- b) An interface with a hand-held receiver and display system of the size of a smart phone. An enforcement officer could use this smart phone like device to measure the weight of each passing vehicle.

Due to the low cost of the sensor, its battery-less zero energy operation and remote hand held display, the enforcement system could be widely deployed if its performance is evaluated to be satisfactory. This was the primary motivation for this research project.

## II. AMR SENSORS FOR VEHICLE DETECTION

### 2.1 VEHICLE DETECTION

The use of anisotropic magnetoresistive (AMR) devices was originally proposed for this project due to the fact that the WIM sensor measures axle weights and can count axles, but sometimes may not be able to calculate the total weight of each vehicle correctly. When two vehicles of the same type travel close together with a small inter-vehicle distance, it may be difficult to identify which axles belong to which vehicle and therefore total vehicle weight calculation may not be possible. The AMR sensors are extremely small sensors that can count vehicles (similar to inductive loops) and therefore could supplement the WIM sensor [4], [5].

An anisotropic magnetoresistive (AMR) sensor has a silicon chip with a thick coating of piezoresistive nickel-iron [4]. The presence of an automobile in close range causes a change in magnetic field which changes the resistance of the nickel-iron layer. Each AMR device provides a voltage proportional to the magnetic field experienced by it.

The 3-axis HMC 2003 set of AMR devices from Honeywell were utilized for the experimental tests described below. Figure 1 shows a printed circuit board (PCB) with two AMR sensors, a PIC-brand microprocessor and a wireless transceiver system that was developed.



**Figure 2.1: PCB with two AMR sensors, microprocessor and wireless transceiver system**

The AMR sensors were clearly able to generate a signal corresponding to the magnetic field of each vehicle and were able to count vehicles. The Appendix to this chapter shows plots of AMR sensor responses to several vehicles.

The signals from the AMR sensors were also utilized to obtain vehicle speed and perform vehicle classification.

### 2.2 VEHICLE SPEED CALCULATION

Two AMR sensors separated by a distance of 10 cm longitudinally were used. A separation of only 10 cm means the two AMR sensors can be placed on a single PCB resulting in a very compact sensor package. The velocity of each passing vehicle is determined by measuring the time delay between the signals of the two AMR sensors. The delay is calculated by taking the cross correlation between the signals of the two AMR sensors and finding the time when the cross-correlation is maximized. Knowing the time delay and the distance between the two AMR sensors, the velocity of the approaching vehicle is estimated.

Table 2.1 and Table 2.2 summarize the results of velocity estimation. In Table 2.1, a sonar sensor was also used to determine the time interval that the vehicle stayed over the sensors.

Knowing the length of the test vehicles, an estimate of the actual velocity can be obtained from the sonar sensor for comparison.

**Table 2.1: Vehicle Velocity Estimation and Reference Sonar Sensor**

Test No.	Test Cars	Sonar Velocity (m/s)	Estimated Velocity (m/s)	Error (%)	Sonar Velocity Upper Bound (m/s)	Sonar Velocity Lower Bound (m/s)	Correlation Coefficient
2	Honda Accord	3.165	3.115	1.592	3.273	3.064	0.978
5	Ford Ranger - 1	4.065	3.585	11.800	4.245	3.899	0.985
6	Ford Ranger - 1	4.017	3.585	10.752	4.193	3.855	0.991
7	Kia Sedona	1.458	1.520	4.283	1.480	1.436	0.992
8	Kia Sedona	1.513	1.597	5.557	1.537	1.489	0.991
10	Kia Sedona	5.998	6.129	2.193	6.396	5.646	0.956
11	Mazda Protégé - 2	1.904	1.919	0.823	1.945	1.863	0.983
12	Mazda Protégé - 2	4.077	3.878	4.903	4.275	3.898	0.981
13	Mazda Protégé - 2	6.165	6.552	6.280	6.627	5.763	0.979
14	Mazda Protégé - 2	3.343	3.800	13.656	3.475	3.222	0.922
15	Mazda Protégé - 2	2.625	2.500	4.751	2.705	2.549	0.971
16	Ford Ranger - 2	2.342	2.235	4.575	2.401	2.287	0.989
17	Ford Ranger - 2	2.774	2.714	2.154	2.857	2.696	0.986
18	Ford Ranger - 2	5.970	5.938	0.546	6.367	5.620	0.982
19	Ford Ranger - 2	6.367	6.786	6.576	6.821	5.970	0.981
20	Ford Ranger - 2	9.279	10.000	7.769	10.275	8.459	0.982
21	Ford Ranger - 2	11.032	11.176	1.307	12.469	9.893	0.973

The sonar sensor had an update rate of 50 milli-seconds (0.05 secs) which caused a considerable error when calculating velocities from the sonar signal. The sonar velocity upper and lower bounds in Table 2.1 are calculated by replacing  $dt$  from sonar with  $(dt + 0.05)$  and  $(dt - 0.05)$ .

Results of Table 2.2 are obtained from tests in which the AMR sensors were sampled at 2 KHz. These tests were done simultaneously with WIM tests and therefore the time interval between the two axels touching the WIM sensors could be measured. Knowing this time interval and the distance between axles for the test vehicles, an estimate of velocity can be obtained for comparison.

**Table 2.2: Vehicle Velocity Estimation with More Accurate Reference Sensor**

Test No.	Test Vehicle	Axel Length (m)	dt - WIM (sec)	Velocity - WIM (m/s)	Velocity 2 - WIM (m/s)	Est. Velocity (m/s)	Error (%)
27	Ford Ranger - 3	2.893	0.298	9.708	10.810	11.111	2.788
31	Ford Ranger - 3	2.893	0.273	10.597	11.800	12.121	2.725
32	Ford Econoline	3.658	0.412	8.884	9.682	9.756	0.770
33	Ford Econoline	3.658	0.444	8.245	8.985	9.091	1.175
34	Ford Econoline	3.658	0.434	8.426	9.182	8.889	3.192
35	Ford Econoline	3.658	0.446	8.192	8.927	8.696	2.591
36	Ford Econoline	3.658	0.434	8.430	9.186	9.091	1.038
37	Ford Econoline	3.658	0.462	7.917	8.627	8.511	1.354
39	SnowPlow	4.801	1.801	2.665	2.847	2.899	1.799
40	SnowPlow	4.801	1.501	3.199	3.418	3.419	0.026
43	SnowPlow	4.801	0.887	5.413	5.784	5.797	0.233
44	SnowPlow	4.801	0.904	5.312	5.675	5.634	0.734

**Summary:** From Table 2.2, it is clear that vehicle speed can be measured with an accuracy of 3% or better using the AMR sensors. As a comparison, consider the speed measurement accuracy offered by loop detectors. From single loop detectors, speed can be estimated with an accuracy of 5-10 mph [7]. With dual loop detectors, speed can be estimated with an accuracy of 1-2 mph [7]. The dual-loop accuracy is comparable to or slightly better than the AMR estimated accuracy at highway speeds, but lower than AMR-estimated accuracy at low road speeds.

## 2.3 VEHICLE CLASSIFICATION

By estimating the velocity of the passing vehicle, and measuring the time duration for which the vehicle's magnetic field stays above a minimum threshold, the vehicle's magnetic length can be calculated. The magnetic length is likely to be close to the actual physical length of the vehicle. Hence, vehicle length can be obtained from the AMR sensors and can be used for vehicle classification.

Table 2.3 summarizes the results with two different thresholds, 35 and 50 counts on X and Z axis measurements of the sensors.

**Table 2.3: Vehicle Magnetic Lengths**

Test No.	Test Cars	Estimated Velocity (m/s)	Eff. Length 35 X (m)	Eff. Length 35 Z (m)	Eff. Length 50 X (m)	Eff. Length 50 Z (m)
2	Honda Accord	3.1148	6.0863	5.8393	5.7633	5.8393
5	Ford Ranger - 1	3.7255	5.3702	4.8325	5.0260	4.8325
6	Ford Ranger - 1	3.5849	5.4256	4.8344	5.0807	4.8344
7	Kia Sedona	1.5833	7.3791	5.8526	6.9277	5.8526
8	Kia Sedona	1.6379	6.7898	5.4393	6.3595	5.4393
10	Kia Sedona	6.7857	6.9413	5.4593	6.4727	5.4593
11	Mazda Protege - 2	1.9192	6.7819	5.6732	6.3974	5.6732
12	Mazda Protege - 2	3.8776	6.5595	5.5462	6.2157	5.5462
13	Mazda Protege - 2	6.7857	6.7184	5.5936	6.3232	5.5936
14	Mazda Protege - 2	3.7255	6.2779	5.2171	5.8583	5.2171
15	Mazda Protege - 2	2.4675	6.2917	5.2386	5.8900	5.2386
16	Ford Ranger - 2	2.3171	5.8980	5.6839	5.4217	5.6839
17	Ford Ranger - 2	2.7941	5.8997	5.6678	5.4166	5.6678
18	Ford Ranger - 2	5.7576	6.3577	5.7000	5.4223	5.7000
19	Ford Ranger - 2	6.7857	6.4255	6.2355	5.8727	6.2355
20	Ford Ranger - 2	10.0000	6.6120	5.6240	5.4973	5.6240

21	Ford Ranger - 2	11.1765	7.1250	6.3333	6.0167	6.3333
22	SafeTruck	11.1765	44.1222	40.6178	42.6867	40.6178
23	SafeTruck	10.0000	49.8644	45.6422	47.9222	45.6422
24	SafeTruck	15.8333	40.5650	37.0975	38.6175	37.0975
26	Ford Ranger - 3	8.6957	6.2000	5.2074	4.2704	5.2074
27	Ford Ranger - 3	10.8108	6.5421	5.5000	4.4526	5.5000
29	Ford Ranger - 3	11.4286	6.3231	5.3231	4.3128	5.3231
30	Ford Ranger - 3	12.1212	5.8976	4.9805	4.0439	4.9805
31	Ford Ranger - 3	12.9032	6.0579	5.0789	4.1368	5.0789
32	Ford Econoline	10.2564	8.1696	7.3565	7.4739	7.3565
33	Ford Econoline	9.5238	7.6250	7.3750	7.1042	7.3750
34	Ford Econoline	9.5238	7.3061	7.0163	6.8408	7.0163
35	Ford Econoline	9.0909	7.6000	7.1755	7.0000	7.1755
36	Ford Econoline	9.0909	7.5833	6.8875	6.9417	6.8875
37	Ford Econoline	8.6957	7.2923	7.0615	6.8154	7.0615
39	SnowPlow	2.9630	9.9770	8.4486	9.4095	8.4486
40	SnowPlow	3.5714	9.6819	8.1890	9.1276	8.1890
41	SnowPlow	3.6036	9.7694	8.2323	9.2065	8.2323
42	SnowPlow	3.9604	9.6609	8.1913	9.0922	8.1913
43	SnowPlow	6.0606	9.8521	8.3315	9.2822	8.3315
44	SnowPlow	5.8824	10.1041	8.5233	9.5068	8.5233

From Figure 2.2, it can be seen that the AMR sensors can clearly distinguish the Navistar tractor trailer from the other much shorter vehicles.

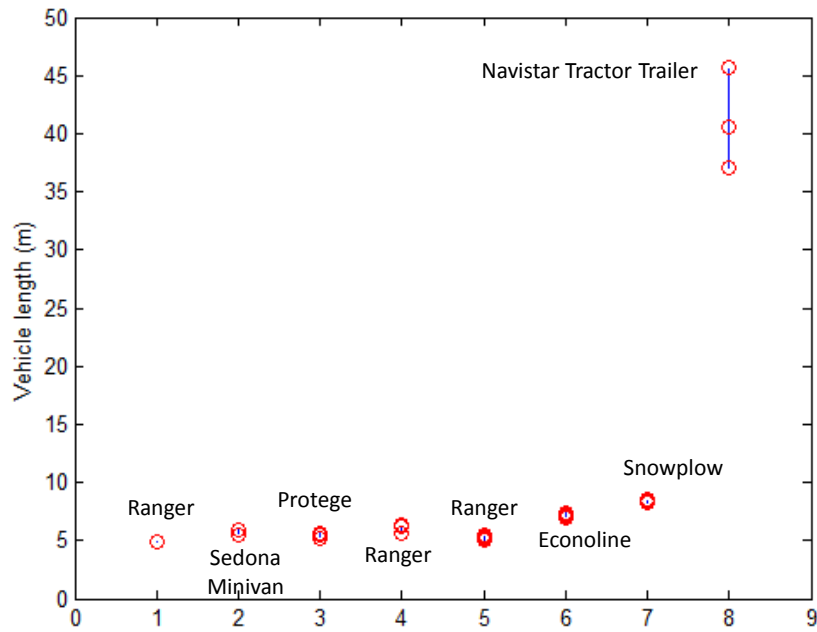


**Figure 2.2: Vehicle lengths estimated by AMR Sensors**

From, Figure 2.3, it can be seen that the AMR sensors can also pick out the snowplow and the Ford Econoline vehicles clearly from the Ford Ranger and the passenger sedans.

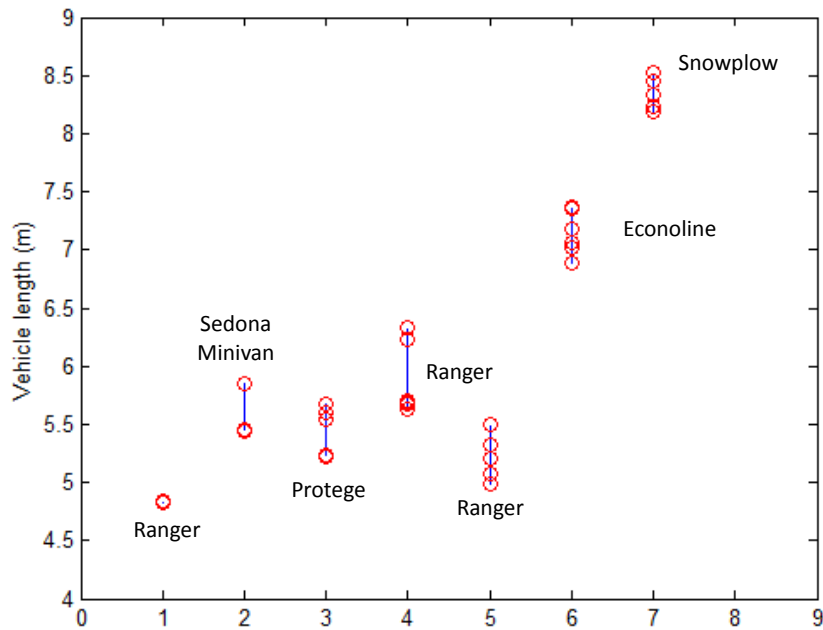


**Figure 2.3: Vehicle lengths estimated by AMR Sensors**

## **2.4 SUMMARY**

Our tests show that the AMR sensors can provide reliable vehicle separation (detection of individual vehicles without regard to the number of axles). Further, they can also provide estimates of vehicle speed and vehicle length. While the AMR sensors would be a good supplement to the WIM sensor, they need additional power for operation. In the case of the battery-less, wireless WIM sensor which operates by energy harvesting, additional power would need to be harvested by using larger piezoelectric stacks. This is not worthwhile, since we have been told by MnDOT that axle weights are the variables of concern, not the total weight of the vehicle. Currently, the developed AMR sensor system is a compact wireless system that can do vehicle counting and classification, but needs to be supplied power.



## 2.5 APPENDIX: SAMPLE MAGNETIC SIGNALS

In this section some of the AMR sensor magnetic signals from different tests are presented.

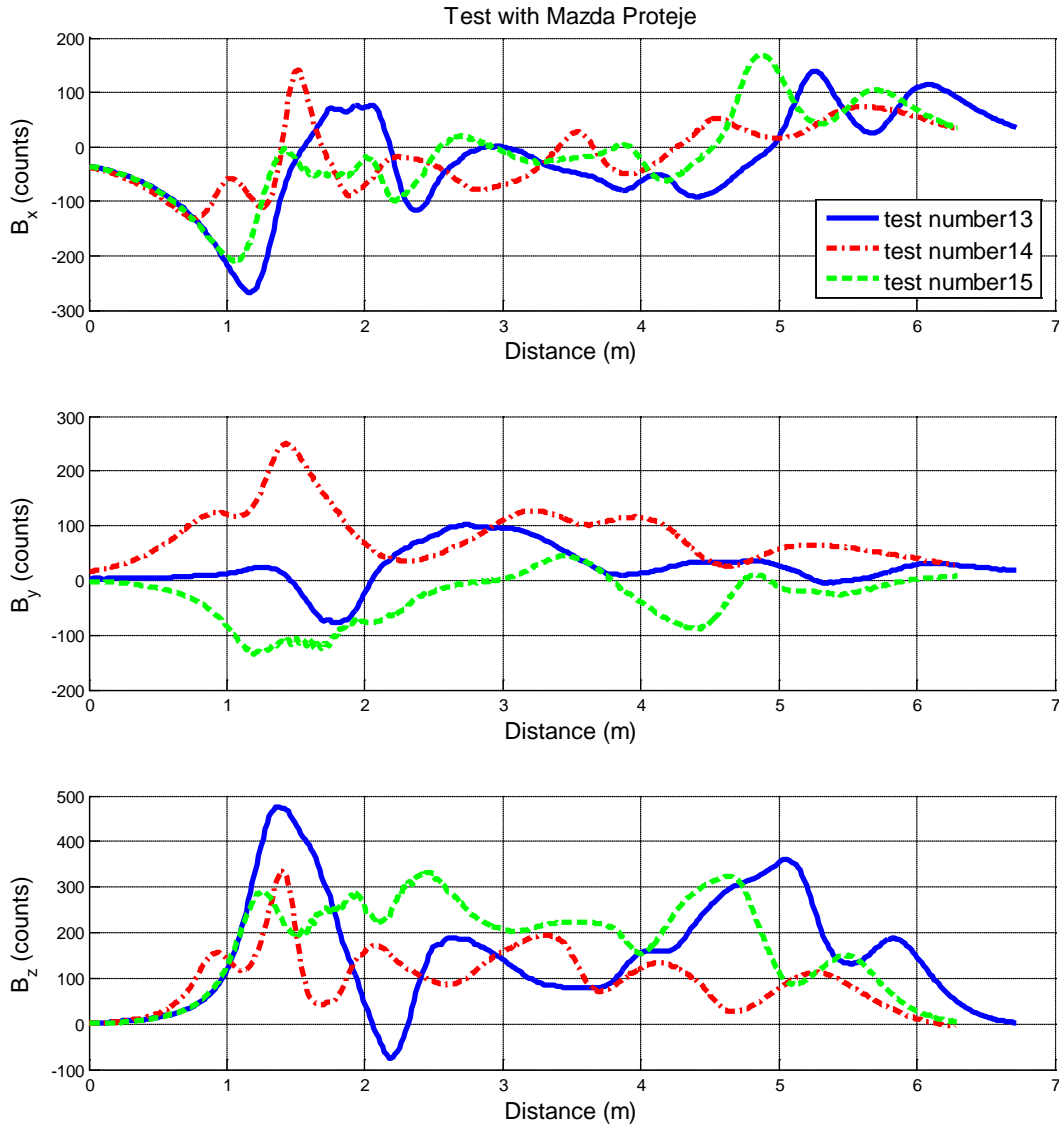


**Figure 2.4: AMR sensor signals with a Mazda Protégé passenger sedan**

In test 14 the vehicle passed over the sensor in a way that the sensor was very close to the right side of the car. In test 15 the vehicle passed over the sensor in a way that the sensor was very close to the left side of the car.

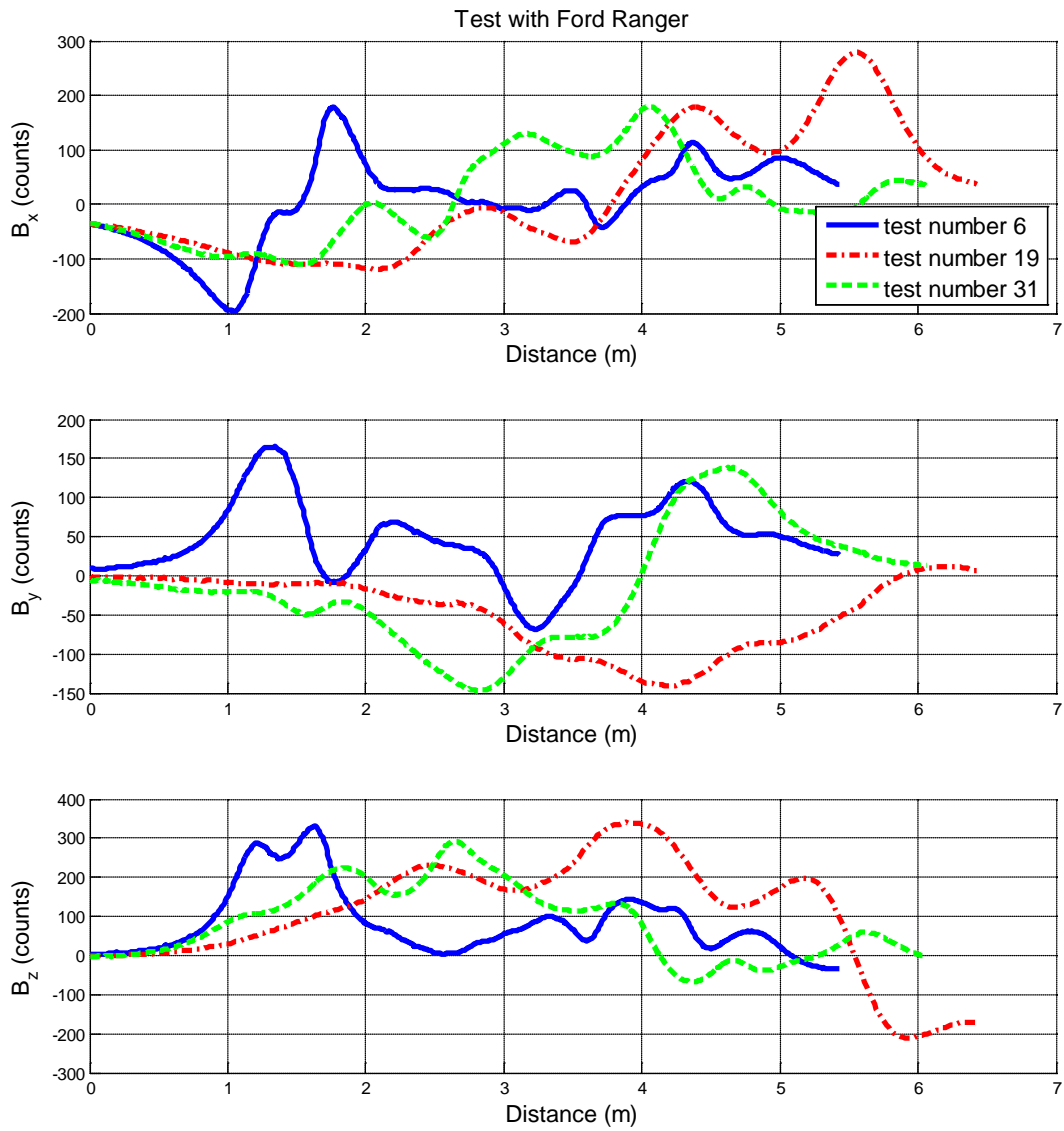


**Figure 2.5: AMR sensor signals with a Ford Ranger small pick-up truck**  
 This test was done at a different geographic location from MnROAD.

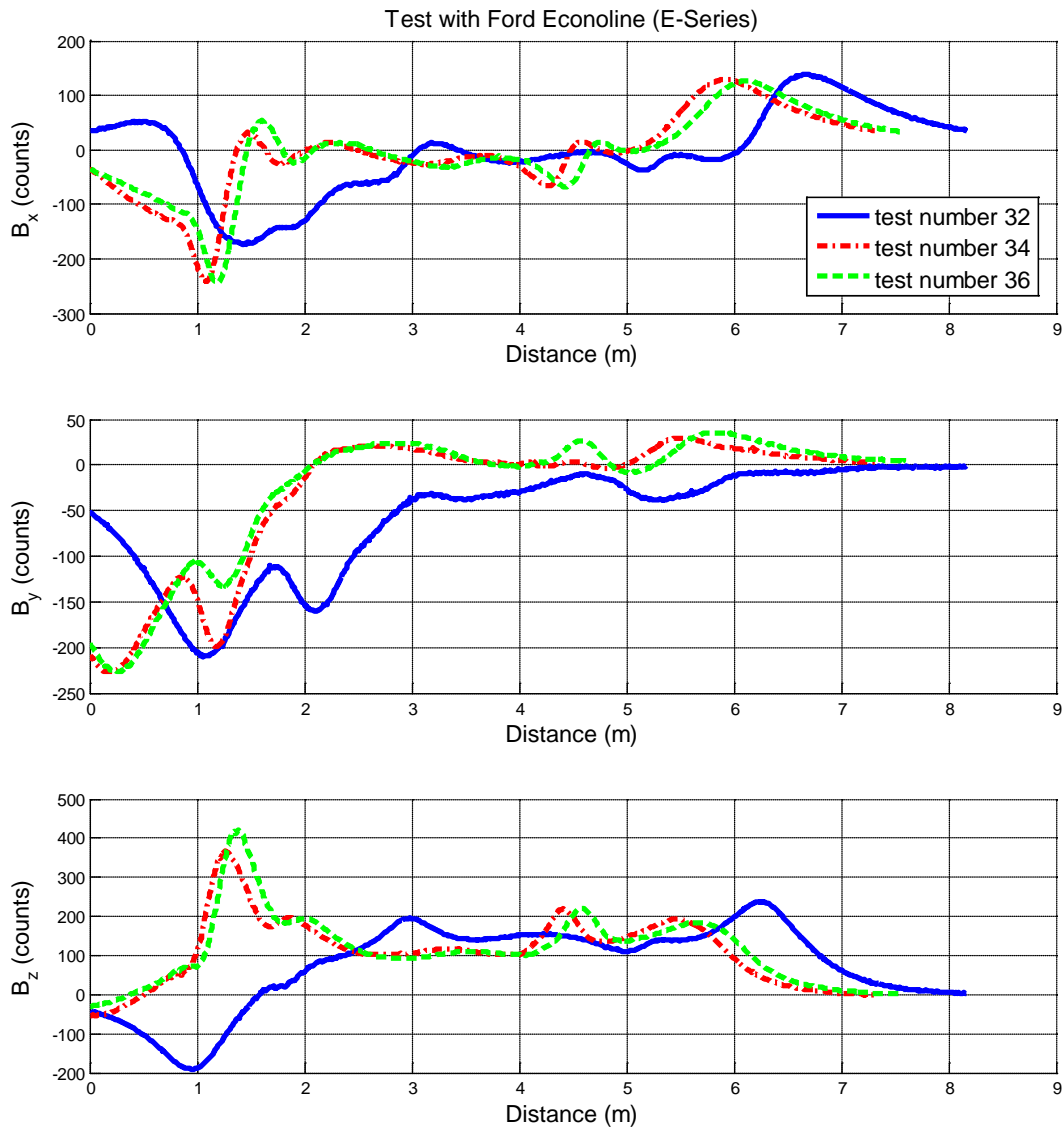


**Figure 2.6: AMR sensor signals with a Ford Econoline E-Series van**

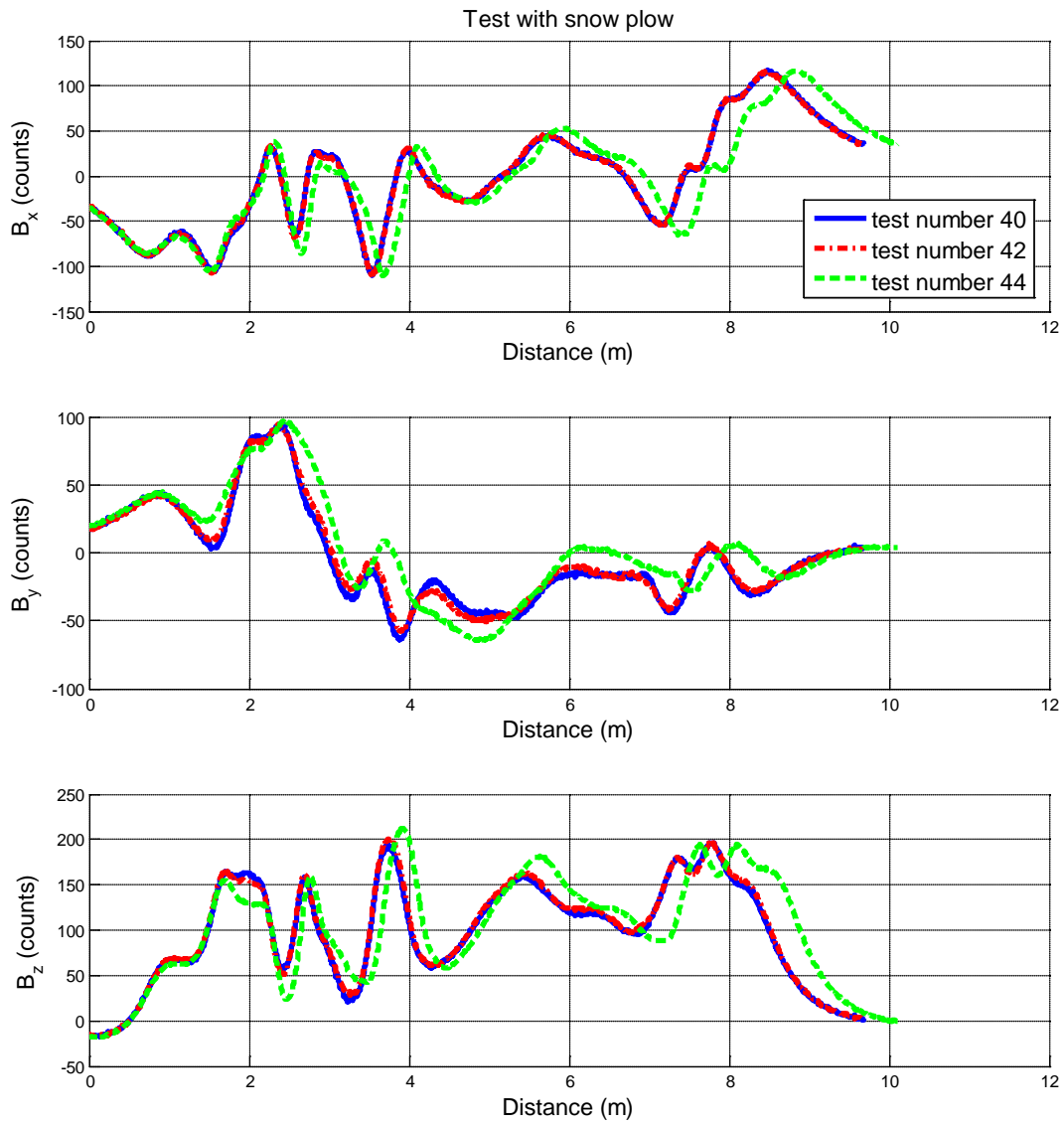


**Figure 2.7: AMR sensor signals with a snowplow**

The tested snow plow vehicle was on the lower end of sizes of snow plows.

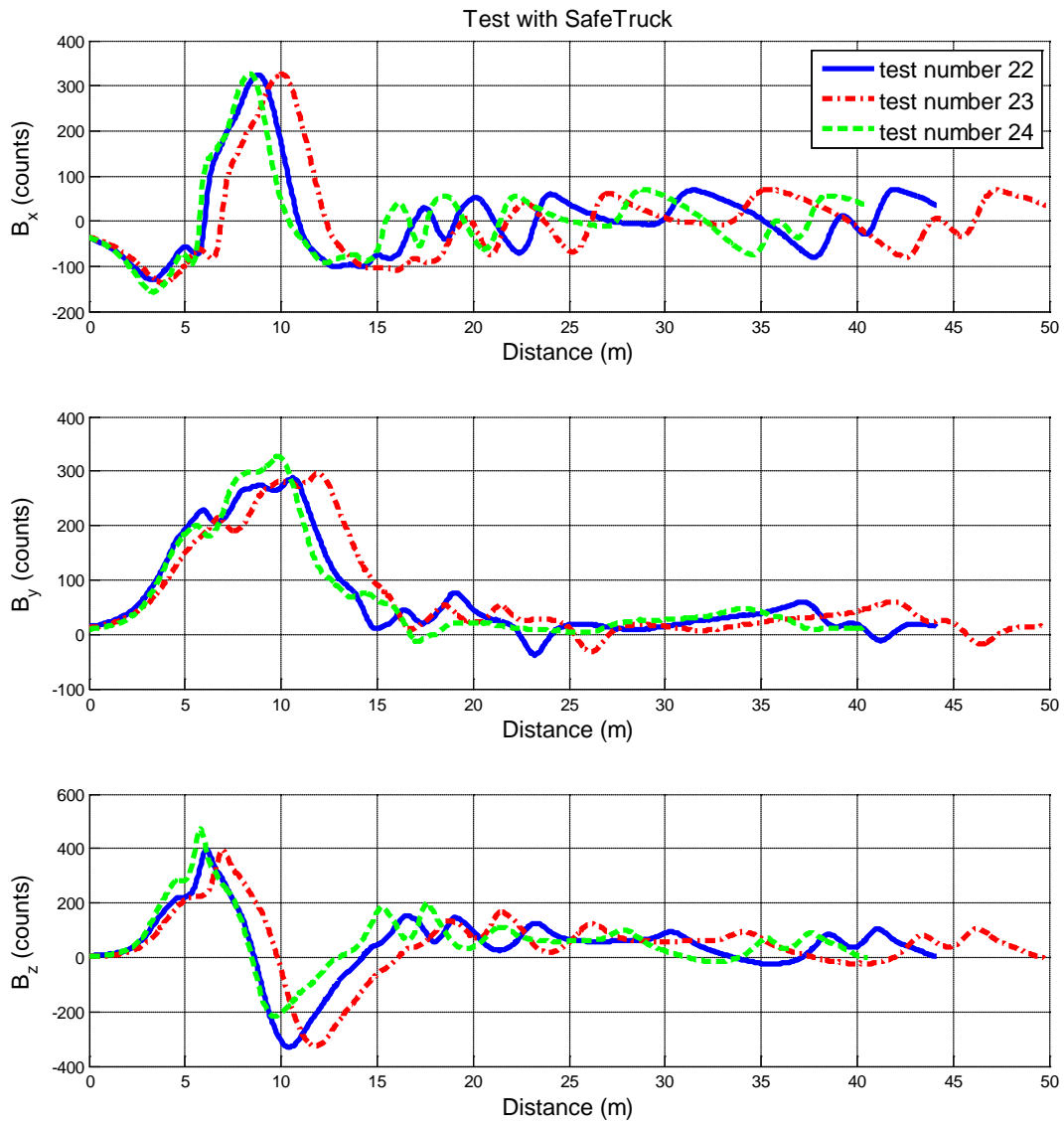


**Figure 2.8: AMR sensor signals with a semi tractor-trailer**

### III. WIM SENSOR REDESIGN

#### 3.1 INTRODUCTION

The weigh-in-motion (WIM) sensor was first re-designed at the beginning of this project while retaining the architecture of having one main top body and 4 sensor legs. The re-design was done to achieve the following objectives:

- 1) Reduce the height of the sensor to 3.5 inches so as to enable its use in an asphalt pavement.
- 2) Replace bending motion of PZT cantilevered beams with compressive motion of a piezo stack. This reduces the amount of vertical deflection in the sensor during vehicle loading.

In addition, using funding from the IDEA program [3], the top of the sensor was converted to be all-metal, instead of having a baler belt top. This would enable the sensor to be more robust to heavy normal vehicle loads and shear forces.

#### 3.2 FIRST GENERATION REDESIGN

The first objective was achieved by moving the legs of the sensor into the main body. The main body of the sensor consists of a rectangular steel channel with four rectangular slots in the lower part of the channel, as shown in Figure 3.1. The four legs slide into these rectangular slots and have adequate height to be able to accommodate the piezos for both energy harvesting and weight measurement, while minimizing the overall height of the sensor.

The reduction in vertical motion of the piezos during vehicle loading minimizes overall sensor motion and helps in installing the sensor into the pavement with grout.

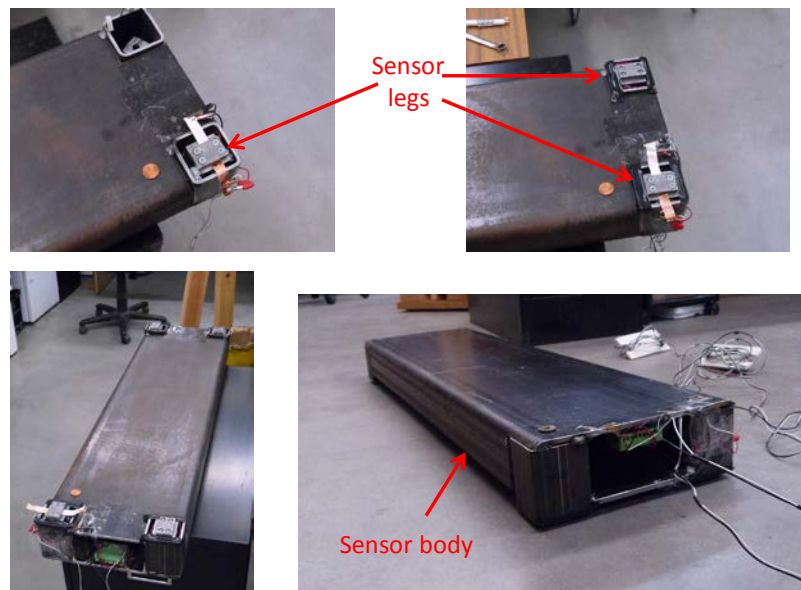


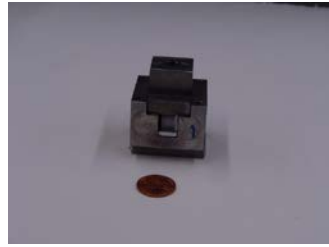
**Figure 3.1: Sensor re-design to move legs into main body of sensor**

A schematic of the overall sensor operation is shown in Figure 3.2. As the truck travels over the sensor, the weight of each axle is measured using piezo transducers and a half wave rectifier. Also energy is harvested using piezo stacks in each of the 4 legs of the sensor. The harvested energy is used to power a microprocessor and a wireless transceiver so that the measured axle weights can be transmitted to a roadside receiver or a handheld display system. The interface system for the roadside receiver and/or handheld display system are described in Chapter 4 of this report. It should be noted that the axle weight is obtained by summing the piezo-obtained force signals from the 4 legs of the WIM sensor. Since total normal (vertical) forces at the 4 legs should sum to the total vertical load exerted on the sensor by each axle, the weight of the axle is obtained independent of the lateral location of the vehicle in the lane.



**Figure 3.2: Schematic of sensor operation**

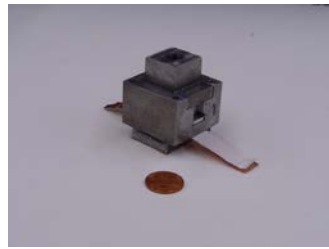
The first generation design of the leg that was pursued is shown in Figure 3.3. Each leg enclosed a piezo stack and a piezo film transducer in series. The series arrangement allows both the stack and the film to experience the vehicle load. The voltage generated in the stack is used to power all of the electronics, while the voltage generated in the film is used to measure the vehicle weight, after additional electronic processing.



Sensor Leg



Piezoceramic for weight measurement



Assembly of Sensor Leg



Assembly of WIM Sensor

**Figure 3.3: First generation sensor leg design**

### 3.3 PERFORMANCE OF FIRST GENERATION SENSOR

The sensor design performed well in being able to measure vehicle weight. Figures 3.4, 3.5, 3.6, 3.7, 3.8 and 3.9 show a Mazda Protégé sedan, a Ford Ranger pick-up truck, a larger Ford pick-up truck, a Ford E-series van, a snowplow and a semi tractor-trailer respectively, that were used for testing with the WIM sensor.

## Mazda Protégé 1999

Approximate total weight = 1800lb

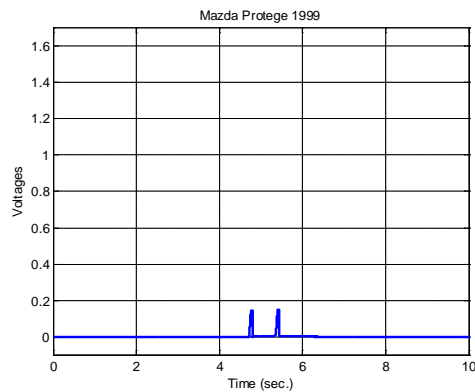


**Figure 3.4: Mazda Protégé sedan used for testing and its sensor response**



# Ford Ranger 2003

Approximate total Weight = 3000 lb

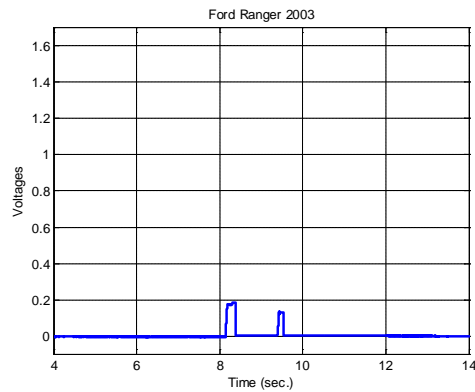


**Figure 3.5: Ford ranger pick-up used for testing and its sensor response**

# Ford Pickup

Approximate total Weight = 6000 lb

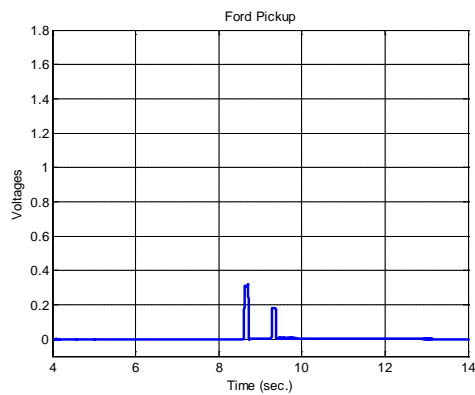


**Figure 3.6: Large Ford pick-up truck used for testing and its sensor response**

# Ford E Series Van

Approximate total Weight = 6000 lb

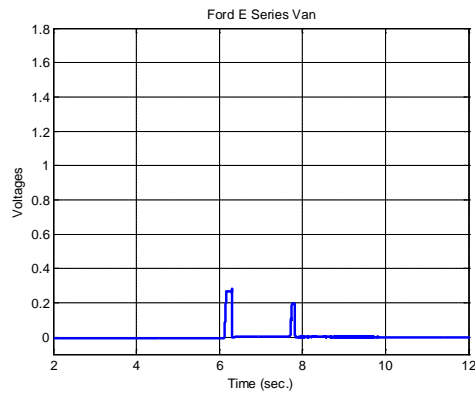


**Figure 3.7: Ford E-series full size van used for testing and its sensor response**

# Snow Plow Truck

Approximate total Weight = 10000 lb

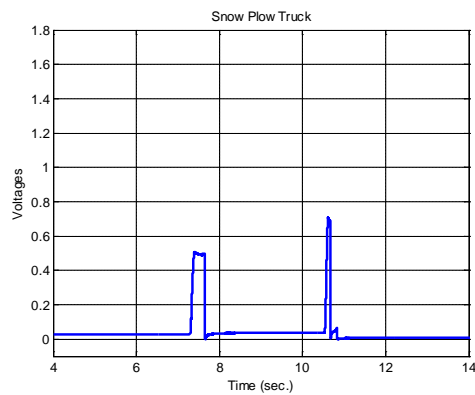


**Figure 3.8: Snowplow truck used for testing and its sensor response**

# Semi-Trailer Truck

Approximate total Weight = 45000 lb

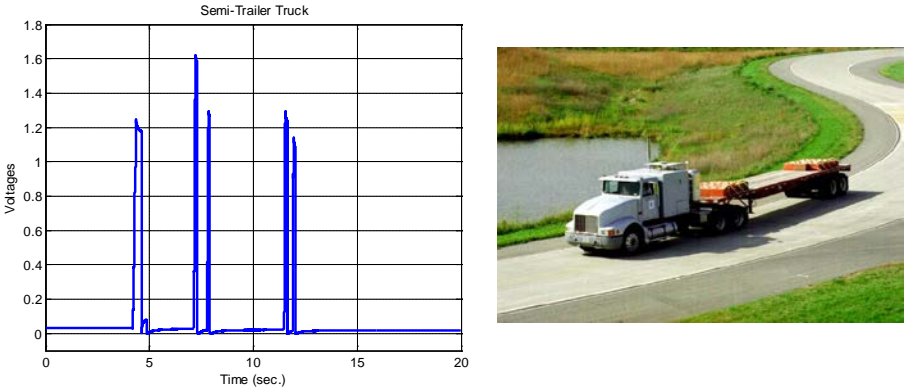


**Figure 3.9: Semi tract-trailer used for testing and its sensor response**

The voltage signal provided by the sensor was a monotonically increasing function of vehicle weight. The voltage versus approximate weight per axle is shown in Figure 3.10

## Approximate Weight Per Axle vs. Voltage

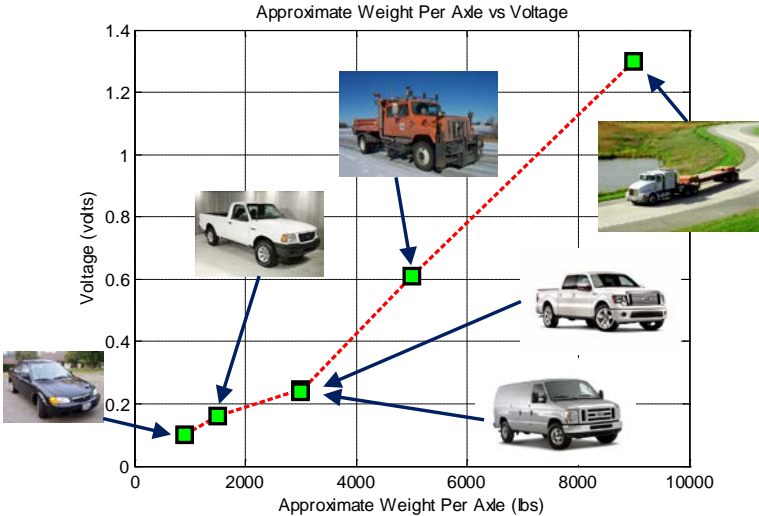


**Figure 3.10: Sensor signal as a function of vehicle weight**

It is clear from the above results that

- a) Adequate energy is harvested even from the smaller vehicles using the piezo stacks for both weight measurement and wireless transmission.
- b) The sensor generated voltage signal increases monotonically with vehicle axle weight. Hence a one-to-one relationship between voltage and weight can be utilized for automatic weight determination.

However, it was also found that the piezo stack often failed (cracked) and had to be replaced. This was judged to be due to excessive loads on the piezo when the semi tractor-trailer traveled over the sensor. The stacks mostly failed when testing with the semi tractor-trailer. Figures 3.11 and 3.12 show photographs of the failed piezo stack.

Hence a re-design of the sensor leg was taken up, so as to prevent excessive forces on the piezo stack when the heaviest vehicles travel over the sensor. This re-design is discussed in section 3.4.

### Problems with Original Leg Design

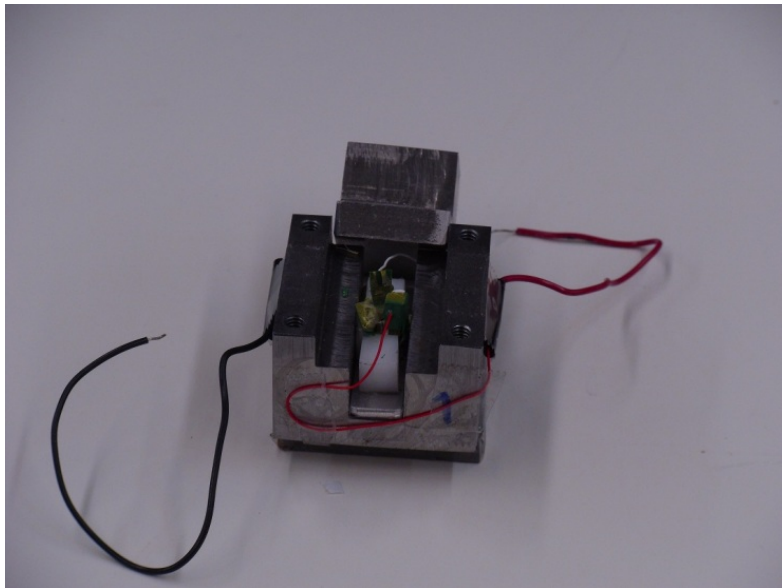


**Figure 3.11: Failures in piezo stack due to semi tractor-trailer loads**

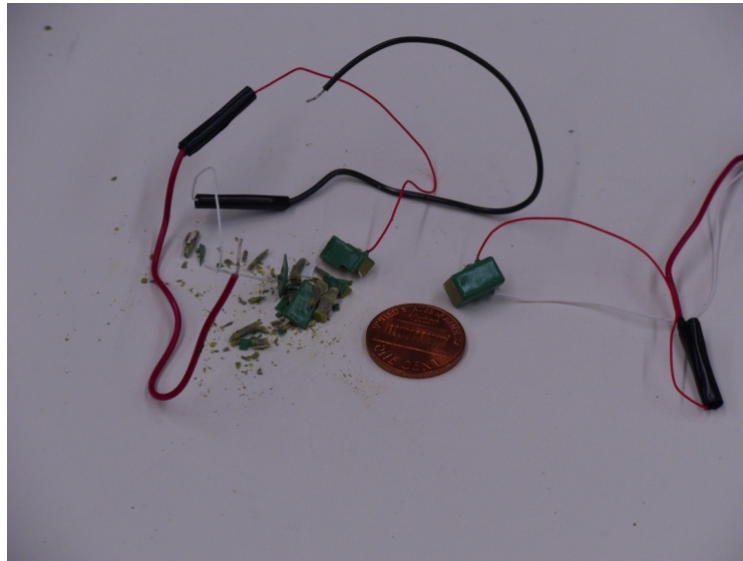


**Figure 3.12: Failures in piezo stack due to semi tractor-trailer loads**

### **3.4 SECOND GENERATION SENSOR REDESIGN**

A schematic of the original design of the sensor leg is shown in Figure 3.13. The piezo stack is located below a steel piston and shims are used to adjust its height above the surrounding housing. The piezo film used to measure vehicle weight is in series and is located below the housing tube, as seen in Figure 3.13. The problem with this design is that the piezo stack experiences the full load of each axle and it is difficult to control the height of the shim to adjust the height of the stack above the housing. The shim should not be too small for adequate energy harvesting from small vehicles, but should not be too high for preventing excessive loads from the semi tractor-trailer.

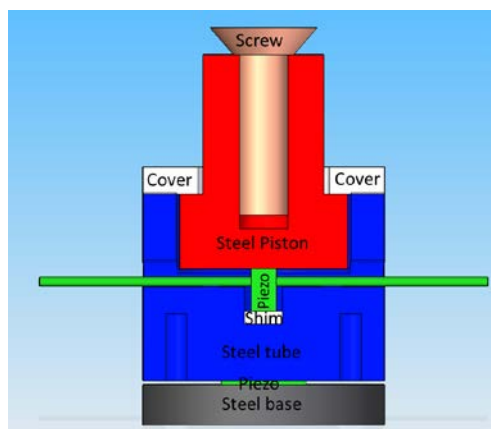
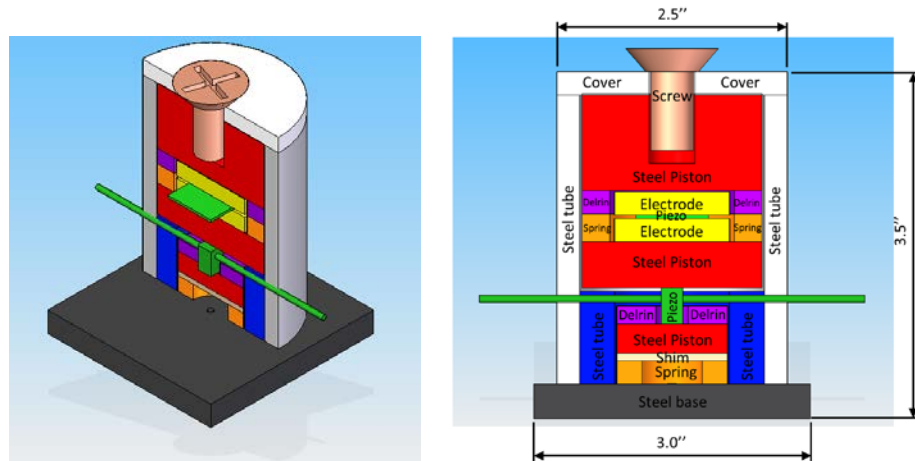


**Figure 3.13: Original leg design (first generation)**



Excess load is prevented by piezo stack getting displaced below the steel tube stops  
 A Bellville washer is added as a spring below the piezo stack

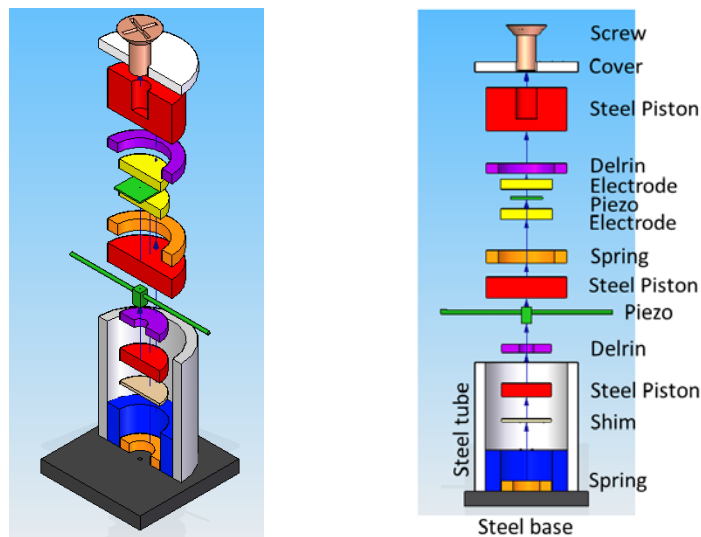
**Figure 3.14: Second generation sensor leg design**

Figure 3.14 shows a schematic of the new leg design. The piezo film for weight measurement is located between top and bottom electrodes. Delrin washers and Bellville springs are placed in parallel with the weight measurement piezo. The piezo film thus experiences a controlled fraction of the vehicle axle weight. At the same time, the voltage generated electronically from the piezo remains proportional to the weight.

The piezo stack is also located in series with Bellville springs. The springs are less stiff than the piezo stack. They allow the piezo stack to move with applied vehicle load and to avoid further loading after adequate displacement is generated to move below the steel tube housing.

Thus the weight measurement piezo film uses springs in parallel, while the energy harvesting piezo stack uses springs in series to achieve their respective functions, while avoiding excessive loads.

Figure 3.15 shows full details of the components used in the new sensor leg design.



**Figure 3.15: Details of new sensor leg design**

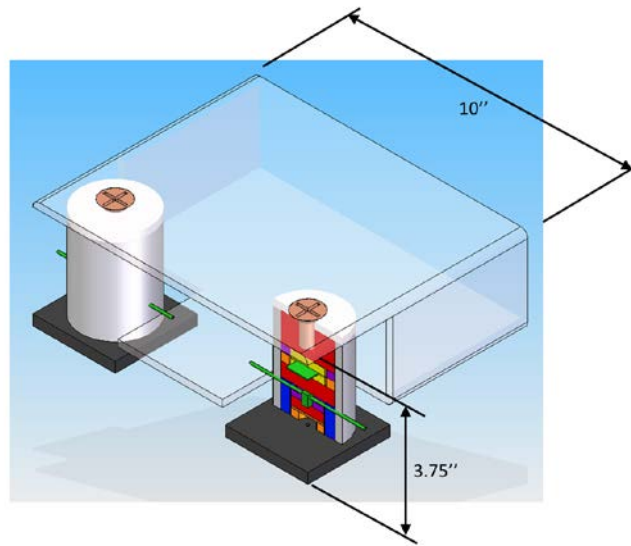


**Figure 3.16: Overall design of second generation sensor showing legs inside main body**

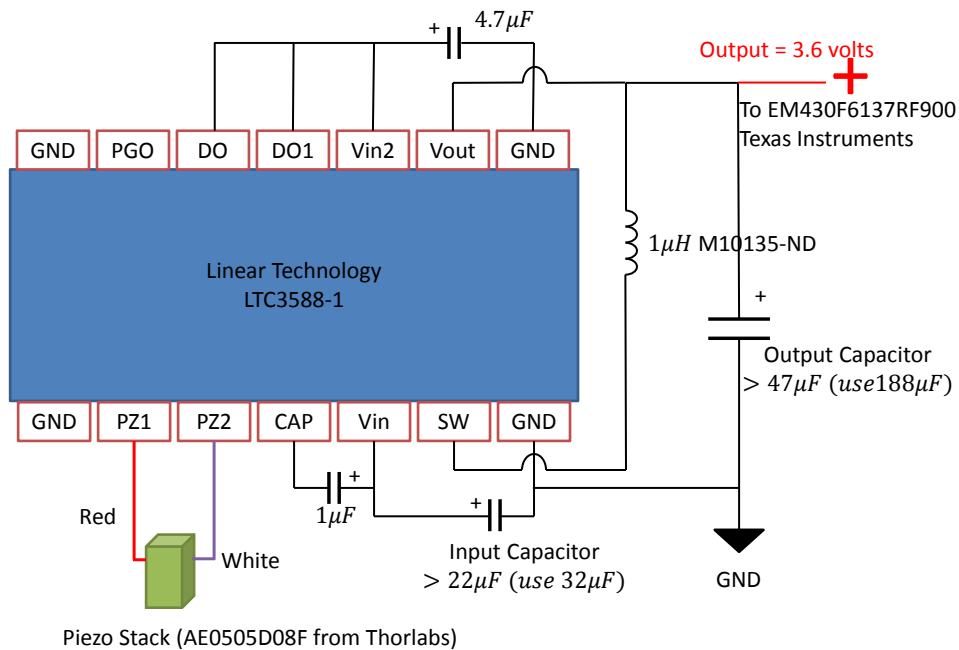
Figure 3.16 shows the overall sensor design, including the sensor legs inside the sensor main body. The new sensor was fabricated and tested. Photographs of the new sensor and its performance in weight measurement are presented in Chapter 5 of this report. The use of a sensor casing to protect the sensor and allow grouting to the pavement is also discussed in Chapter 5.

## IV. ELECTRONIC AND SOFTWARE INTERFACES

### 4.1 ELECTRONICS INSIDE WIM SENSOR

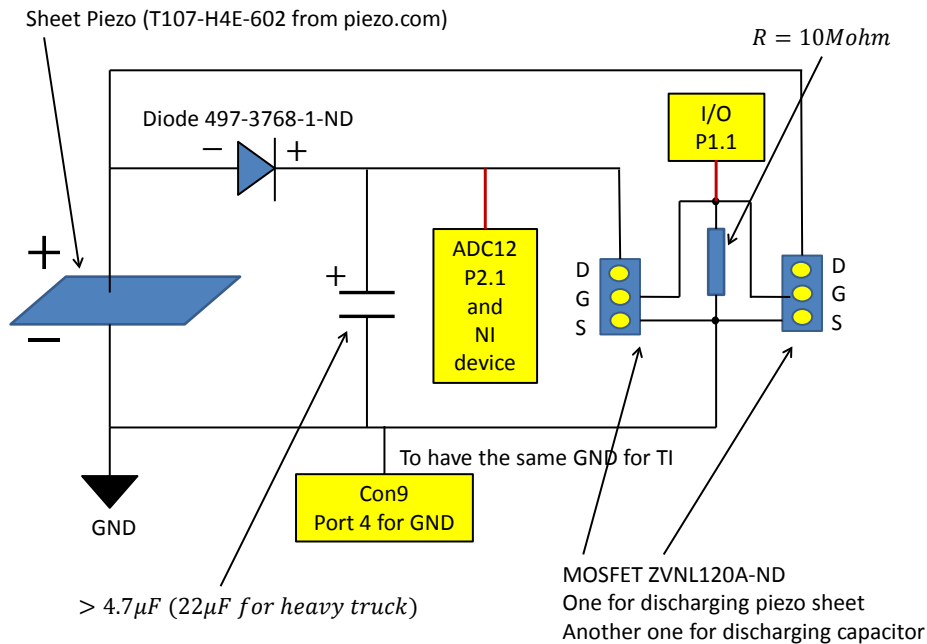
Figure 4.1 shows the electronic circuit used for harvesting energy from the piezoelectric stack. The circuit uses the Linear Technology LTC3588-1 chip. The piezo stack AE0505D08F from Thor Labs is used as the energy generation element. The mechanical design for accommodating the piezo electric stack in the legs of the WIM sensor was discussed earlier. The input capacitor in the circuit is used to store energy after rectification of the voltage from the piezo stack. The output capacitor receives power from the input capacitor, after the voltage on the input capacitor has adequately built up. A built-in voltage regulator on the LTC chip ensures that a constant voltage of 3.6 volts is supplied across the output capacitor. This output port supplies the energy required for the weight measurement and wireless transmission circuits.

Figure 4.2 shows the circuit used to measure the weight of each axle. The voltage from the sheet piezo is passed through a half-rectifier and used to charge a weight measurement capacitor. The voltage across the capacitor is proportional to the charge generated in the piezo and hence the weight of the axle. MOSFETs and the CC430 microprocessor [6] are used to discharge the capacitor after the voltage across it has been measured and before the next axle loads the sensor.



**Figure 4.1: Energy harvesting circuit that interfaces with piezoelectric stack**





**Figure 4.2: Weight measurement circuit that uses piezo film and charge amplifier circuit**

## 4.2 SOFTWARE INTERFACES

Figure 4.3 shows the 3 major interface components developed. The first box (from the left) is a wireless range extender that is placed within 75 feet of the WIM sensor. It receives wireless weight readings from the WIM sensor and then transmits the message to the MnDOT intranet through a router in the IRD controller box. The range extender has a range of 1 mile. The second box shown in Figure 4.3 is the handheld wireless display system. It directly receives wireless weight readings from the WIM sensors and displays axle weights. Figure 4.5 shows a close-up of the handheld display system. The third box in Figure 4.3 is the box inside the IRD controller that receives messages from the wireless range extender. It contains a wireless Digi International XBee Pro transceiver and an Arduino microprocessor. Wireless data is received using the transceiver. The Arduino processor sets up a web site on which the data is displayed. This web site is accessible using any laptop that can connect with the MnDOT intranet. Figure 4.4 shows the internals of the components inside the range extender, the handheld wireless display and the wireless receiver. The wireless handheld LCD display contains 5 lines of text and has the ability to show up to 5 axles of a vehicle on one screen. Additional axles/vehicles can be accessed by scrolling up and down on the display.



**Figure 4.3: Major interface components for access to WIM sensor**



**Figure 4.4: Showing internals of interface components for WIM sensor**



**Figure 4.5: Close-up of wireless handheld display**

Figure 4.6 shows readings from a downloaded file of sensor readings downloaded from the WIM sensor web site over the MnDOT intranet.

[Download!](#)

Wireless

Weigh in Motion

Date	Time	Weight
4/15/2013	22:40:26	8246 lb
4/15/2013	22:40:28	8246 lb
4/15/2013	22:40:29	8246 lb
4/16/2013	14:31:46	7645 lb
4/16/2013	14:32:24	7645 lb
4/16/2013	14:32:25	7645 lb
4/17/2013	8:51:4	7890 lb b
4/17/2013	8:51:6	7890 lb b
4/17/2013	8:51:7	7890 lb b
4/17/2013	8:51:8	7890 lb b
4/17/2013	8:51:10	7890 lb
4/17/2013	9:42:49	7890 lb
4/17/2013	9:42:49	7890 lb
4/17/2013	9:42:50	7890 lb
4/17/2013	9:42:51	7890 lb
4/17/2013	9:42:51	7890 lb
4/17/2013	9:43:12	7890 lb
4/17/2013	9:43:13	7890 lb
4/17/2013	9:43:14	7890 lb
4/17/2013	9:43:15	7890 lb
4/17/2013	10:19:18	7890 lb
4/17/2013	10:19:19	7890 lb
4/17/2013	10:19:20	7890 lb
4/17/2013	10:19:22	7890 lb
4/17/2013	10:19:23	7890 lb
4/17/2013	10:19:27	7890 lb
4/17/2013	10:19:28	7890 lb
4/17/2013	10:19:29	7890 lb
4/17/2013	10:19:29	7890 lb
4/17/2013	10:19:30	7890 lb
4/17/2013	10:21:6	3324 lb
4/17/2013	10:30:45	17192 lb
4/17/2013	10:33:48	lb lb

Figure 4.6: Downloaded file of WIM sensor readings

## V. EXPERIMENTAL RESULTS

### 5.1 SENSOR GROUTING IN PAVEMENT

The weigh-in-motion sensor has undergone multiple revisions in design since the start of this project, as discussed in Chapter 3. The final major design objectives achieved are as follows:

- 1) The use of double-layered sensor legs that fit into vertical slots in the main sensor body allowed the sensor height to be reduced to 3.5 inches.
- 2) The use of bellville washers for springs in parallel and in series with the WIM measurement piezos has allowed weigh-in-motion measurements without saturation over a wide range of axle weights.
- 3) Protection of piezo stacks from over-loads at high-speed operation: Steel tubes are used to support vehicle weight and protect piezo stacks from further loads once allowable piezo stack deformation is exceeded.
- 4) Initially a baler belt was used as the sensor top to cover the components of the sensor and at the same transmit load to the sensor. Later, an external all-metal box was developed in which the sensor is placed (using funds from an IDEA-Program funded project [3]). Bending deformations of the top metal plate transmit vehicle load to the sensor. Grouting the external all-metal casing still allows motion of the sensor inside the casing.

A photograph of the grouted metal casing with the sensor inside is shown below in Figure 5.1.

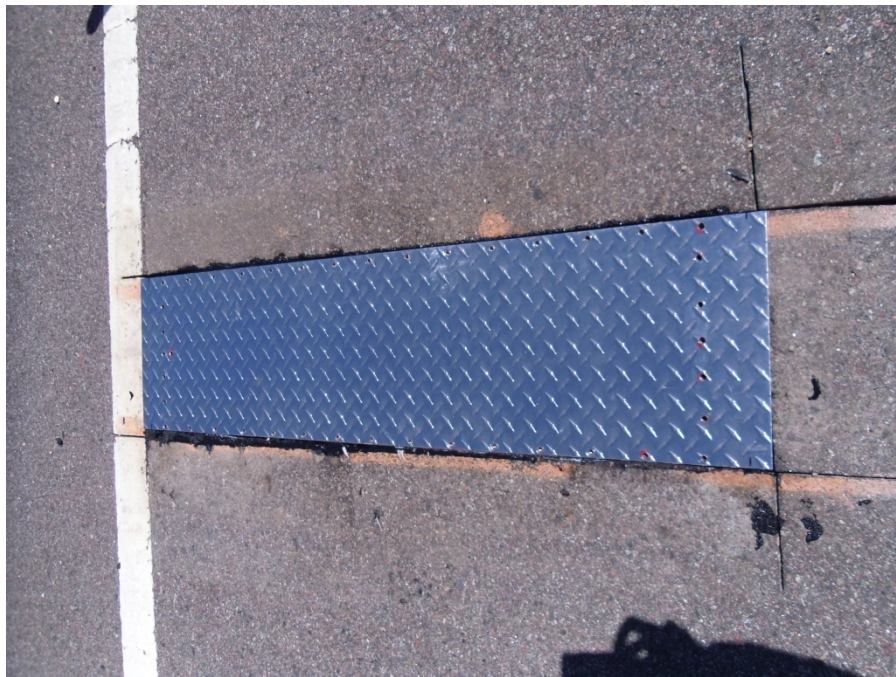


**Figure 5.1: Photograph of sensor in external box that has been grouted in asphalt pavement**

## 5.2 AXLE WEIGHT READINGS

The weigh-in-motion measurements of the sensor for various vehicles are shown in Figure 5.2 below for speed from 0-40 mph. The vehicles used in the tests are a small pick-up, a mini-van, a large pick-up, a snowplow, and a 5-axle 80,000 pound semi truck. The weights shown are half-axle weights. Raw sensor signals were shown earlier in Chapter 3. Figure 5.3 shows half-axle weights for the same vehicles for the speed range 0-50 mph.

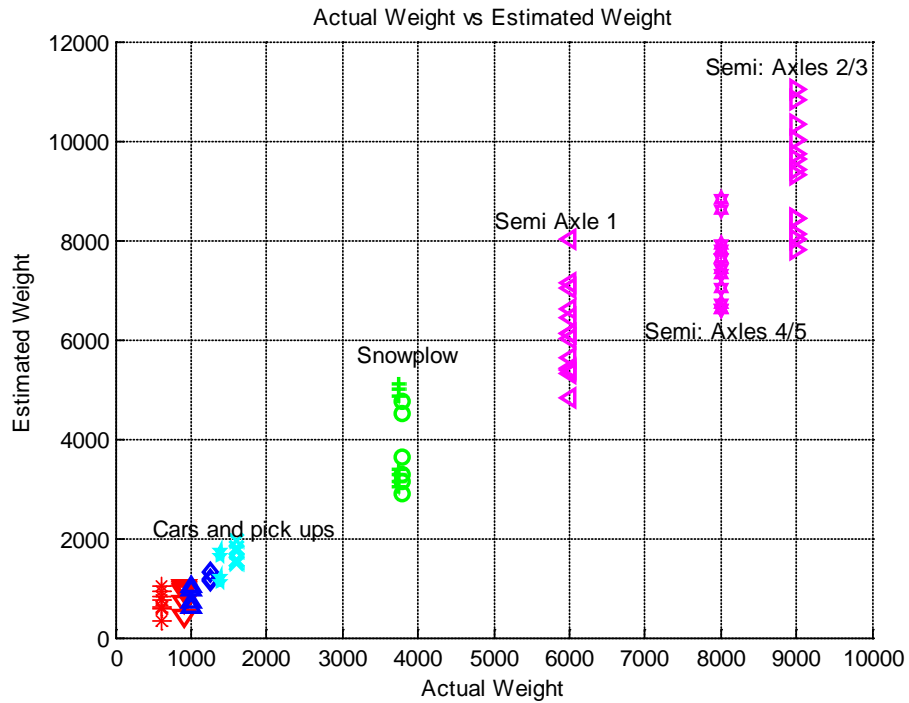
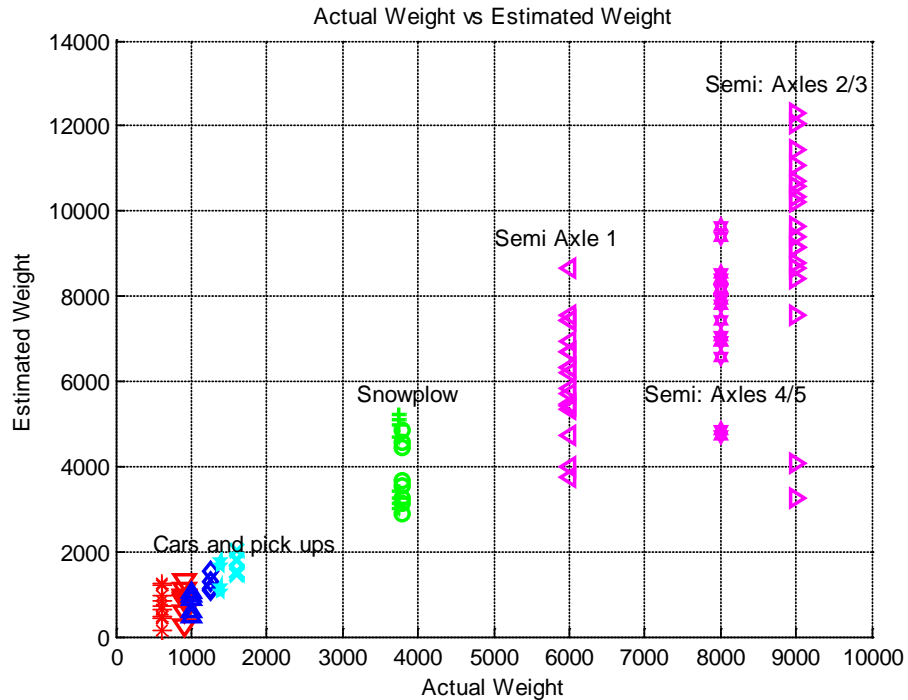


Figure 5.2: Half Axle weight measurements for various vehicles at speeds from 10 – 40 mph



**Figure 5.3: Half Axle weight measurements for various vehicles at speeds from 10 – 50 mph**

### 5.3 TRUCK VIBRATIONS

It can be seen that there is a significant spread in the weight measurements for the semi-truck and that this spread is worse for the 10-50 mph speed range compared to the 10-40 mph speed range. We feel that the spread is due to vibrations in the truck suspension (In other words, the large variations in weight are due to actual variations in load on the sensor resulting from dynamic suspension vibrations).

The figures below (Figures 5.4 – 5.8) show axle vibrations on the first and second axles of the semi-truck at speeds ranging from 10 mph to 50 mph. It can be seen that vibrations are low at 10 mph (< 100 milli-g's rms), increase to 500 mg rms at 40 mph and increase significantly to 900 mg rms at 50 mph.

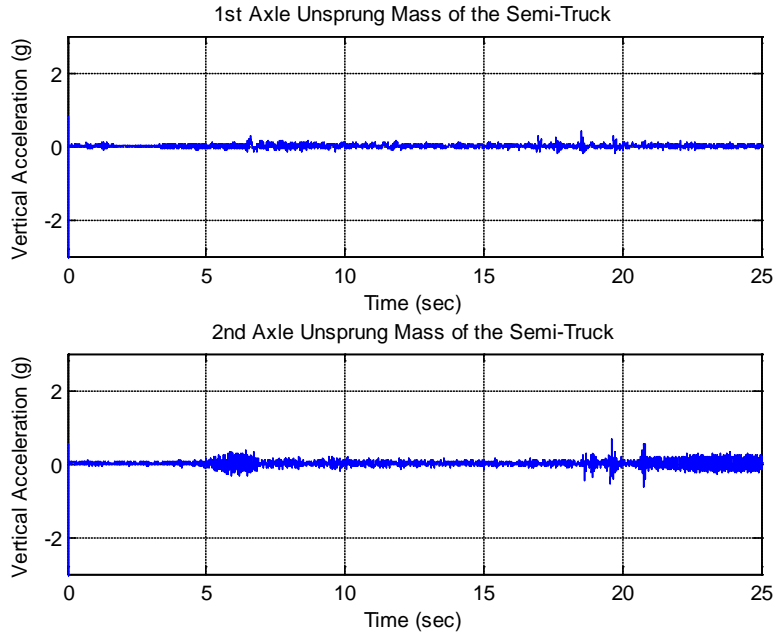


**Figure 5.4: Axle vibrations on semi truck at 10 mph**

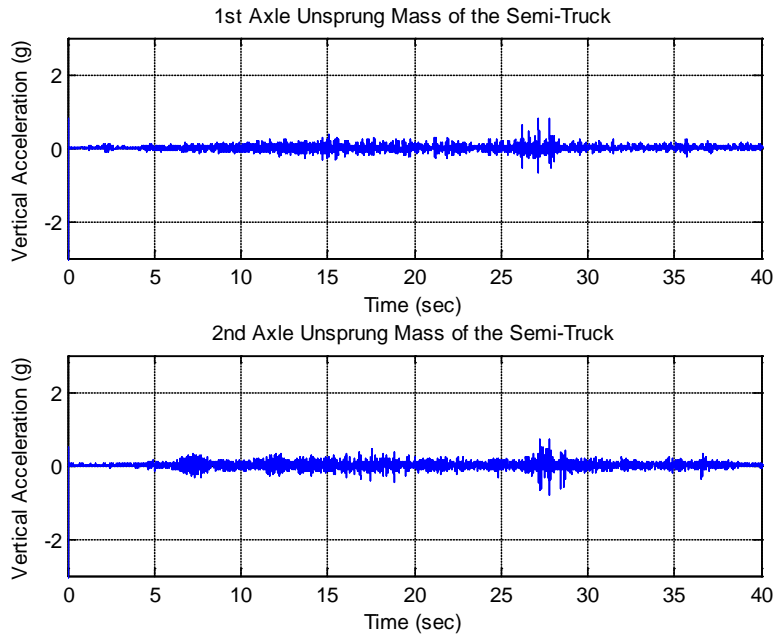


**Figure 5.5: Axle vibrations on semi truck at 20 mph**



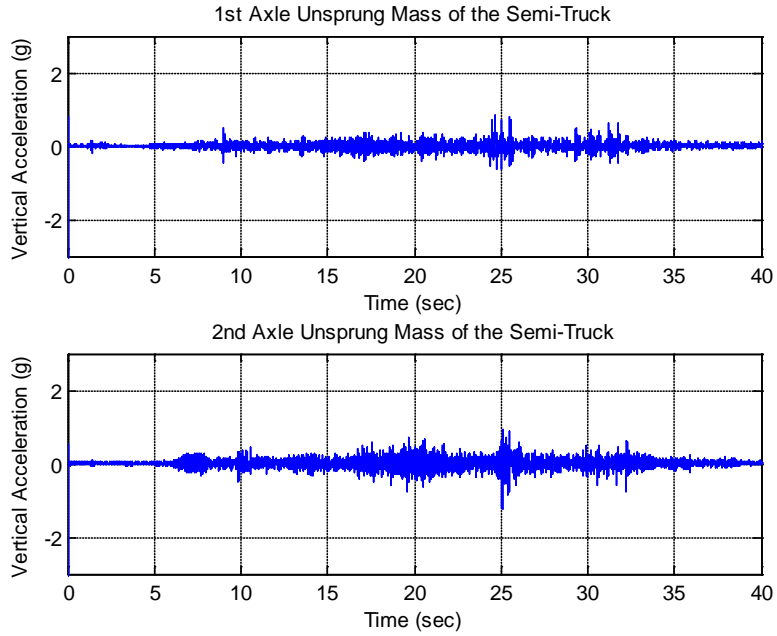


**Figure 5.6: Axle vibrations on semi truck at 30 mph**

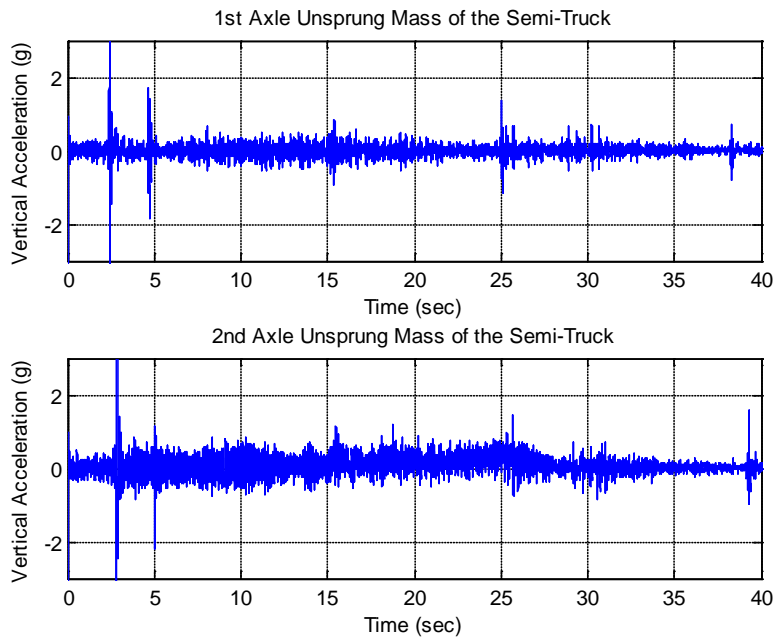


**Figure 5.7: Axle vibrations on semi truck at 40 mph**

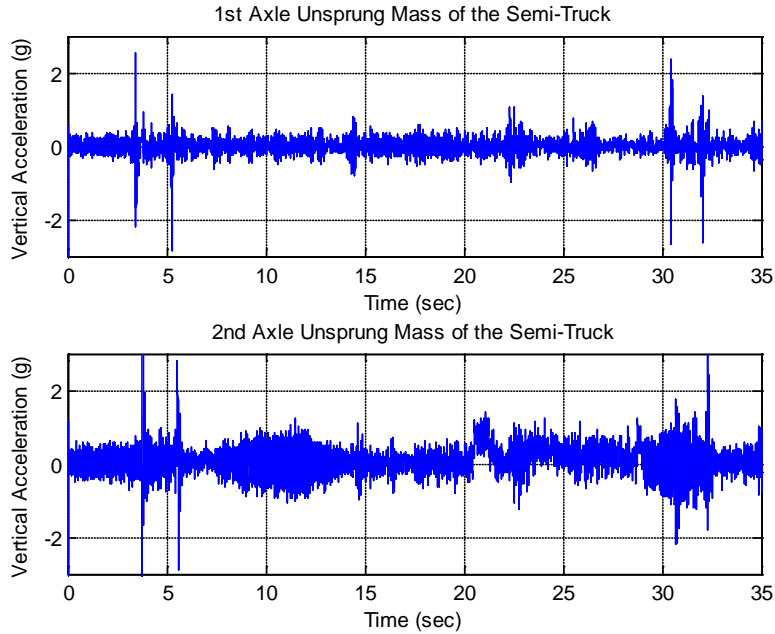


**Figure 5.8: Axle vibrations on semi truck at 50 mph**

#### **5.4 SUMMARY**

The sensor has a monotonically increasing voltage response to vehicle weights. However, there is significant variation in the weight measurement from one test run to another test run for the same vehicle. At the same time, there are also significant vibrations in the truck suspensions, as seen in the vibration data collected by using accelerometers on the truck axles. The vibrations are as much as 500 mg rms at 40 mph and increase to 900 mg rms at 50 mph. Due to the high vibrations measured on the truck axles, variations in measured axle weight are to be expected.

## VI. CONCLUSIONS

This project made significant improvements to the design of a battery-less, wireless weigh-in-motion system. The height of the sensor was reduced from 5 inches to 3.5 inches to enable it to function in an asphalt pavement. The vertical deflections in the sensor were reduced by replacing bending piezo transducer motion with compressive motion of a piezo stack. The sensor was made robust to heavy vehicle loads by an arrangement of parallel and series springs that prevented overloading and also allowed vehicle weight measurement. The electronics in the sensor were also made more robust by using a commercial-off-the shelf power electronics chip from Linear Technologies together with additional circuits designed by the research team.

There was unexplained loss of data for the reading from the first axle of the semi-truck on several occasions. This could not be explained as inadequate energy harvesting, since the energy harvesting system provided adequate energy from the first axle for several much lighter vehicles.

Two types of interface systems were developed:

- a) An interface system that connected to the Internet network inside an IRD controller box so that sensor readings could be accessed through the MnDOT intranet.
- b) An interface system that utilized a wireless handheld display system, from which a nearby user can directly observe the axle-weights of passing vehicles.

At the conclusion of the tasks for interface development, MnDOT felt that the WIM system was not suitable for deployment at a real-world highway location due to its significant weight and width and that there was a risk of it being dislodged from the road and posing a hazard to the vehicles on the road. Hence task 6 in the project (consisting of testing the sensor at a real-world traffic location) was cancelled and the project was ended without this task being taken up. Correspondingly, the budget for the project was reduced by \$15,000 due to elimination of this task.

## REFERENCES

- [1] K. Vijayaraghavan and R. Rajamani, "Ultra Low Power Control System for Maximal Energy Harvesting from Short Duration Vibrations," *IEEE Transactions on Control Systems Technology*, Vol. 18, No. 2, pp. 252-266, March 2010.
- [2] S. Pruden, K. Vijayaraghavan and R. Rajamani, *Enhancement and Field Test Evaluation of New Battery-Less Wireless Traffic Sensors*, Center for Transportation Studies, June 30, 2011.
- [3] R. Rajamani, *Battery-Less Wireless Weigh-in-Motion Sensor*, Proposal funded by the IDEA Program, Project NCHRP-IDEA 165, 2012.
- [4] S. Taghvaeeyan and R. Rajamani, "Portable Roadside Sensors for Vehicle Counting and Speed Measurement," *Proceedings of the 92<sup>nd</sup> Transportation Research Board Annual Meeting*, Washington, DC, January 2013.
- [5] M. J. Caruso and L. S. Withanawasam, "Vehicle detection and compass applications using AMR magnetic sensors," *Proceedings of the Sensors Expo*, 1999.
- [6] Texas Instruments, SLAS554E - CC430F613x Data Sheet, Texas Instruments, Dallas, Texas, November 2010.
- [7] *Traffic Flow Measures Implementation Guide*, Report, Center for Advanced Transportation Technology, University of Maryland, July 2010, available at website: [http://www.catt.umd.edu/sites/default/files/documents/traffic\\_flow\\_measure\\_guidelines\\_v8.pdf](http://www.catt.umd.edu/sites/default/files/documents/traffic_flow_measure_guidelines_v8.pdf).